Sleep Medicine 137 (2026) 108663

Contents lists available at ScienceDirect

Sleep Medicine

journal homepage: www.elsevier.com/locate/sleep

A multimodal 7T MRI and biomarker study reveals reversible brain changes following acute sleep deprivation

Eric Einspänner [a,b,*], Hendrik Mattern [c,d,e], Heiko Grossmann [f], Eya Khadhraoui [a], Sebastian J. Müller [a], Alejandra P. Garza [g], Ildiko R. Dunay [g], Katharina Schregel [h], Charles R.G. Guttmann [i], Erelle Fuchs [a,1], Daniel Behme [a,b,1]

[a] Otto von Guericke University, Medical Faculty, Clinic for Neuroradiology, Magdeburg, Germany
[b] Research Campus STIMULATE, Otto von Guericke University, Germany
[c] Otto von Guericke University, Department of Biomedical Magnetic Resonance, Magdeburg, Germany
[d] German Center for Neurodegenerative Diseases, 39120 Magdeburg, Germany
[e] Center for Behavioral Brain Sciences, Magdeburg, 39120, Germany
[f] Otto von Guericke University, Institute for Mathematical Stochastics, Magdeburg, Germany
[g] Otto-von-Guericke University, Institute of Inflammation and Neurodegeneration, Magdeburg, Germany
[h] University Hospital Jena, Institute of Diagnostic and Interventional Radiology, Section Neuroradiology, Jena, Germany
[i] Harvard Medical School, Brigham and Women's Hospital Department of Radiology, Boston, USA

ARTICLE INFO

Keywords:
Sleep deprivation
Neuroimaging
Biomarkers
7T MRI
PVS

ABSTRACT

Acute sleep deprivation is known to impair vigilance performance and alter brain physiology. This study investigates structural, physiological and cognitive effects of one night of sleep deprivation (SD) and subsequent recovery.

Thirty healthy participants underwent (18M/12F, mean age 28.0 ± 4.7 years, range 20–38) a multimodal assessment including 7T MRI, plasma biomarker analysis, and Psychomotor Vigilance Task (PVT) testing at three time points: baseline, after 24 h of SD, and following a 72-h recovery period.

Our results demonstrate that SD induced a significant increase in total perivascular space (PVS) volume (from 6711.5 mm^3 to 7475.3 mm^3; $p < 0.001$), a marker of impaired glymphatic function, which completely normalized after recovery. These macrostructural changes were accompanied by reversible microstructural alterations, including decreased T1 relaxation times and shifts in quantitative susceptibility mapping (QSM) in multiple brain regions, indicative of dynamic fluid shifts. Systemically, SD led to an increase in pro-inflammatory markers, notably MMP-9 (from 52.3 pg/mL to 69.2 pg/mL; $p < 0.05$), and changes in multiple peripheral biomarkers. Behaviorally, participants exhibited significantly more attentional lapses (slowest 10 % RT: 386.4 ms–410 ms; $p < 0.05$), which were also reversed upon recovery.

In conclusion, a single night of SD triggers a cascade of interconnected and fully reversible physiological changes, likely initiated by transient glymphatic disruption. Healthy individuals are able to recover mostly from one night of SD, suggesting that adverse effects of SD, when not in a chronic state, can potentially be reversed.

1. Introduction

Sleep is fundamental for maintaining brain homeostasis and plays a crucial role in waste clearance, with perivascular spaces (PVS) thought to play a pivotal role in this process [1–4]. This system facilitates the removal of toxins from the brain, with cerebrospinal fluid (CSF) flowing into the PVS and mixing with interstitial fluid (ISF), which then drains through perivenous and periarterial spaces [3–8]. Sleep disturbances,

* Corresponding author. Clinic for Neuroradiology, Otto-Von-Guericke-University Magdeburg, Leipziger Str. 44, D-39104, Magdeburg, Germany.
E-mail addresses: eric.einspaenner@med.ovgu.de (E. Einspänner), hendrik.mattern@ovgu.de (H. Mattern), heiko.grossmann@ovgu.de (H. Grossmann), eya.khadhraoui@med.ovgu.de (E. Khadhraoui), sebastian.mueller@med.ovgu.de (S.J. Müller), alejandra.garza@med.ovgu.de (A.P. Garza), ildiko.dunay@med.ovgu.de (I.R. Dunay), katharina.schregel@med.uni-jena.de (K. Schregel), guttmann@bwh.harvard.edu (C.R.G. Guttmann), erelle.fuchs@ovgu.de (E. Fuchs), daniel.behme@med.ovgu.de (D. Behme).
[1] Contributed equally.

https://doi.org/10.1016/j.sleep.2025.108663
Received 29 September 2025; Received in revised form 29 October 2025; Accepted 9 November 2025
Available online 11 November 2025

ranging from acute deprivation to chronic disorders like insomnia, have well-documented psychophysiological consequences, including impaired vigilance, memory consolidation, and emotional regulation. Traditionally, sleep-related brain alterations have been assessed using electroencephalography (EEG), which reveals changes in brain synchronization and cortical excitability [9–12]. This vital process primarily occurs during sleep, highlighting the importance of adequate sleep for brain health.

Conversely, sleep deprivation is detrimental to health and has been linked to various neurological disorders, including Alzheimer's disease (AD) [13,14]. Animal models further demonstrate that chronic sleep deprivation actively drives neuropathology by triggering potent neuroinflammation via glial cell activation in the hippocampus [15]. This sustained cellular stress impairs synaptic plasticity essential for memory [16] and can ultimately lead to irreversible neuronal injury through mitochondrial damage and apoptosis [17]. A leading theory for these destructive effects on brain health points to the disruption of the brain clearance [5]. Sleep deprivation is known to impact both the immune and glymphatic systems [13,18]. Studies in mice have shown an association between sleep deprivation and the activation of proinflammatory cytokines such as TNF-a [19]. However, a recent meta-analysis of human studies did not find changes in inflammatory proteins after a single night of sleep deprivation [20].

Directly detecting changes in the glymphatic system is challenging [21]. Therefore, PVS enlargement is commonly used as a proxy for assessing glymphatic function [22,23]. PVS can be exquisitely delineated and visually assessed using 7T MRI [24,25] The superior spatial resolution and high signal-to-noise ratio of ultra-high-field MRI are essential for the 'exquisite delineation' and accurate automated and semi-automated segmentation strategies that provide metric and morphological features to estimate the amount of fluid present in the PVS [22,26–28], which is more challenging at lower field strengths [25]. PVS enlargement is also observed in aging and various neurological disorders, although its precise role remains under investigation [18,29–32]. For example, PVS are significantly enlarged in patients with chronic insomnia, who also exhibit signs of cognitive impairment [5].

To date, few human studies have investigated the impact of a single night of sleep deprivation on brain health [33,34]. We aimed to address this gap and further our understanding of sleep deprivation's effects on health, as well as to explore the reversibility of adverse effects. Our study investigates whether short-term sleep deprivation has a measurable negative impact on healthy individuals, and if so, whether these effects are reversible with sleep restoration. We hypothesize that transient adverse effects of sleep deprivation can be observed in healthy individuals, but that these effects can quickly recover once sleep is restored. By examining PVS morphology, peripheral biomarkers, reaction time and expecting changes in tissue composition, this exploratory study seeks to further elucidate the impact of sleep deprivation on PVS and the immune system, both of which are key factors in the development of neurological disorders. While PVS enlargement is a widely used proxy for impaired glymphatic function, it is an indirect measure. A key strength of our study's longitudinal design is that by tracking changes in PVS volume relative to each participant's own baseline, we control for inter-individual confounds in baseline PVS burden, isolating the specific effect of sleep deprivation.

2. Material and methods

2.1. Participants/subjects

Thirty healthy participants were recruited from June 2024–January 2025 and enrolled in this study. Healthy subjects between the ages of 20–40 years, female and male, with any background, left and right handedness were eligible. Participants were recruited from the local university and community via posted flyers and internal mail lists. Contraindications included sleep disorders, such as sleep apnea, medication intake, chronic illnesses, epilepsy, and pregnancy as well as general MRI contraindications such as tattoos, tinnitus, pregnancy, metallic implants, and claustrophobia. As part of this screening, participants completed a questionnaire which included self-reporting on any known sleep problems or sleep disorders (see Table 1, 'Sleep Disorder'). Participants who reported a known sleep disorder were excluded. No further clinical examinations or specific questionnaires were performed. All participants provided written informed consent. The study was approved by the local Ethics Committee (25/24, Addendum April 18, 2024) and conducted according to the Declaration of Helsinki.

2.2. Experimental design

Participants were supervised by medical staff in order to ensure the safety and health of participants, as well as to confirm that the participants were awake for the allocated 24h of sleep deprivation.

The first two MRI scans were taken 24h apart, with a minimum of 24h of sleep deprivation between the first two scans. The third and final MRI scan took place three days after the second scan. Blood samples were also collected at each MRI timepoint. Between the first and second scan, participants were asked to eat and drink normally, and to avoid high-intensity sports activities (short walks were permitted) and only low caffeine intake (less than in everyday consumption). No sleep restrictions were placed between the second and third scan, and participants were asked to eat and drink as they normally would. Exercise was to be kept in moderation. Participants were asked to refrain from alcohol during the testing week. To minimize circadian variations, all three measurement sessions (0h, 24h, 96h) were scheduled at the same time of day for each participant. Blood samples were collected immediately after the MRI scan. The study design is shown in Fig. 1.

2.3. MRI protocol

Images were acquired on a whole body 7T Plus MRI scanner (Siemens Healthineers, Erlangen, Germany; gradient strength: 70 mT/m, slew rate: 200 T/m/s) using a 32-channel receive head coil (8Tx/32Rx), applying equal imaging protocol settings at all time points. Following an initial localizer scan, we acquired a 3D high-resolution T1-weighted magnetization prepared two rapid gradient echo (MP2RAGE) sequence (TR/TE = 4800/2.01 ms, TI_1/TI_2 = 900/2750 ms, matrix size = 320 x 320 x 256, α_1/α_2 = 5/3°, acquisition time = 744 s). For

Table 1
Baseline Demographics and Characteristics of Study Participants (N = 30). Values are presented as mean ± standard deviation or n (%). [1]The value for sleep disorder was constant (2.0) across all participants, indicating no known sleep disorders within the sample.

Characteristic	Value
Age (years)	
Mean ± SD	28.0 ± 4.7
Median	27
Min/Max	20/38
Gender and age distribution	
Men	18 (60 %)
Mean ± SD	27.3 ± 4.6
Median	26
Min/Max	20/37
Women	12 (40 %)
Mean ± SD	29.2 ± 4.9
Median	27.5
Min/Max	23/38
Children (n)	0.17 ± 0.46
Sleep Disorder	All participants reported the same status[1]
Sport per week (sessions)	2.8 ± 1.5
Alcohol consumption (units/week)	0.6 ± 0.6
Alcohol consumption (units/month)	2.4 ± 2.6
Smoker/Non-smoker	2/28

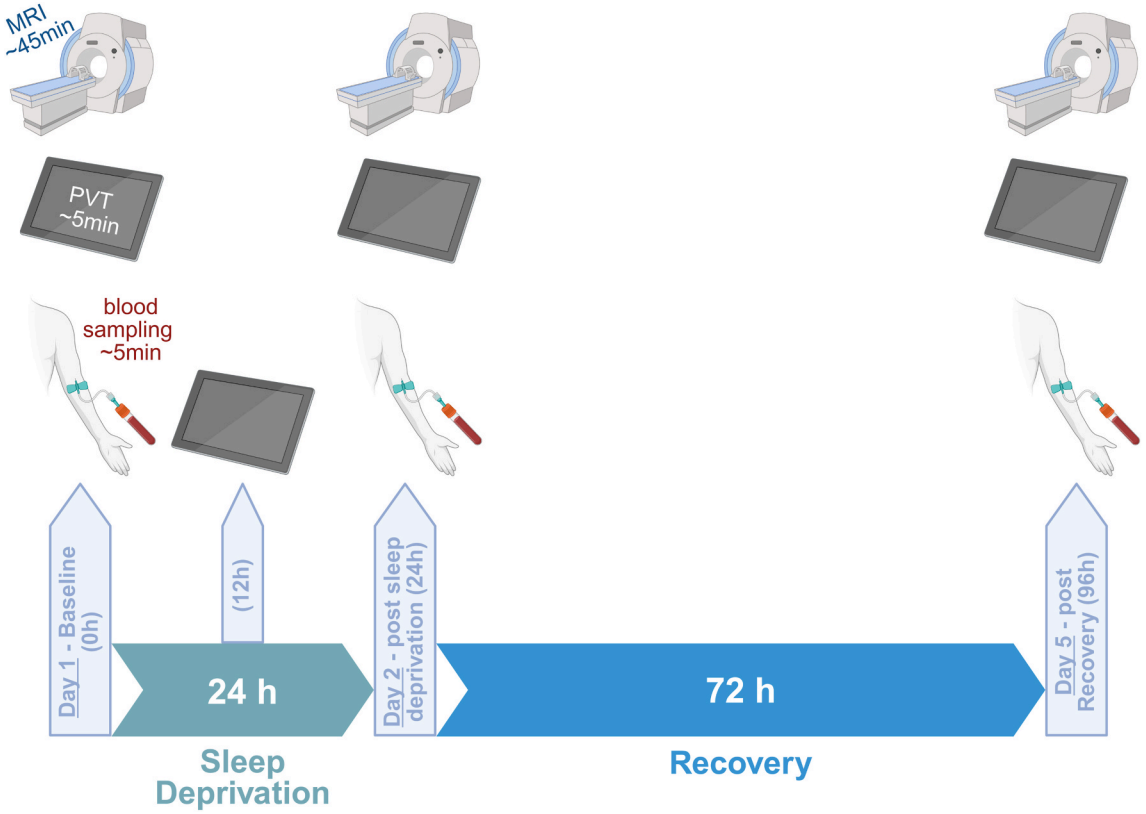

Fig. 1. Experimental study design. The flowchart illustrates the longitudinal study protocol. 7T MRI, the NASA Psychomotor Vigilance Task (PVT) and blood samples, were collected at three primary time points: at baseline, following 24h of total sleep deprivation (SD) and after a recovery phase. An additional PVT was performed midway (12h) through the sleep deprivation period. (This figure was created in https://BioRender.com.).

susceptibility mapping, a 3D multi-echo, ASPIRE-based gradient echo (GRE) sequence [35] was used (TR = 25 ms, TE = 5, 10, 15, 20 ms, matrix size = 320 x 320 x 240, $\alpha = 10°$, acquisition time = 849 s). Finally, a 3D T2-weighted (T2w) SPACE sequence was acquired (TR/TE = 5500/458 ms, matrix size = 320 x 320 x 240, variable $\alpha = 120°$, acquisition time = 479 s). All three sequences had an isotropic spatial resolution of 0.7 x 0.7 × 0.7 mm^3.

2.4. Psychomotor Vigilance Task

The impact of sleep on vigilance performance was measured using reaction time assessments from the Psychomotor Vigilance Task (PVT) [36], conducted four times over the five-day period: twice on day 1 (0h and 12h), once on day 2 (24h), and once on day 5 (96h). The test was performed on a clinic provided iPad (Apple Inc., Cupertino, CA, USA) with the application Nasa PVT+ (NASA Ames Research Center) [37].

2.5. Data analysis

2.5.1. PVS segmentation

For the automated segmentation of PVS, the nnU-Net [38] framework was employed [39,40]. The network was trained using three manually segmented T2w datasets (same sequence as described in Methods) acquired previously from a healthy subject. The detailed procedures for PVS annotation included several steps. Initially, a group meeting was convened to unify opinions regarding the definition of PVS and the visual threshold required for delineating a specific PVS. PVS segmentation was performed by a doctoral student with extensive experience in PVS segmentation (>2 years of experience; various MRI studies). These segmentations underwent group meetings and final corrections by a senior radiologist (>10 years of experience). The observers used 3D Slicer (v5.6.2, https://www.slicer.org) [41] with an oversampling factor of 3 and the level tracing segmentation tool [42] to segment PVS on a voxel basis. Segmentation was initially performed on the sagittal slices (whole brain) and then verified using the axial and coronal slices. To enhance the robustness and generalizability of the model, the training data was substantially increased through data augmentation using the torchio library [43]. The augmentation pipeline included the application of random elastic deformations, simulated bias-field artifacts, motion artifacts, and the addition of random noise. The nnU-Net model was trained using the T2w images as the input channel and the corresponding manual PVS segmentations as the ground truth label maps. Following training, the model was used to generate PVS predictions for all T2w datasets in the study (see Fig. 2). Finally, the PVS volume was calculated for different ROIs (whole brain, white matter, hippocampus and basal ganglia) from these automated segmentations. From all labels available in the Desikan-Killiany-Tourville (DKT) atlas [44,45], we chose these regions as PVS occur most frequently in these regions, thus rendering them most relevant in the context of our study. The PVS values presented here are total volumes from both hemispheres, i.e. left and right white matter, hippocampus and basal ganglia.

2.5.2. QSM and T1

Quantitative Susceptility Maps (QSM) were reconstructed from the multi-echo GRE data using the QSMbox toolbox [46]. Quantitative T1 maps were directly obtained from the MP2RAGE sequence [35]. To perform region-of-interest (ROI)-based analysis, whole-brain segmentation was conducted on the T1-weighted images using FastSurferCNN [47], which provides cortical and subcortical labels based on the DKT atlas. The resulting segmentation masks were then registered to the individual QSM and T1 map spaces using FSL FLIRT [48]. Finally, for each ROI, the mean magnetic susceptibility and T1 relaxation time were calculated and reported as mean ± standard deviation.

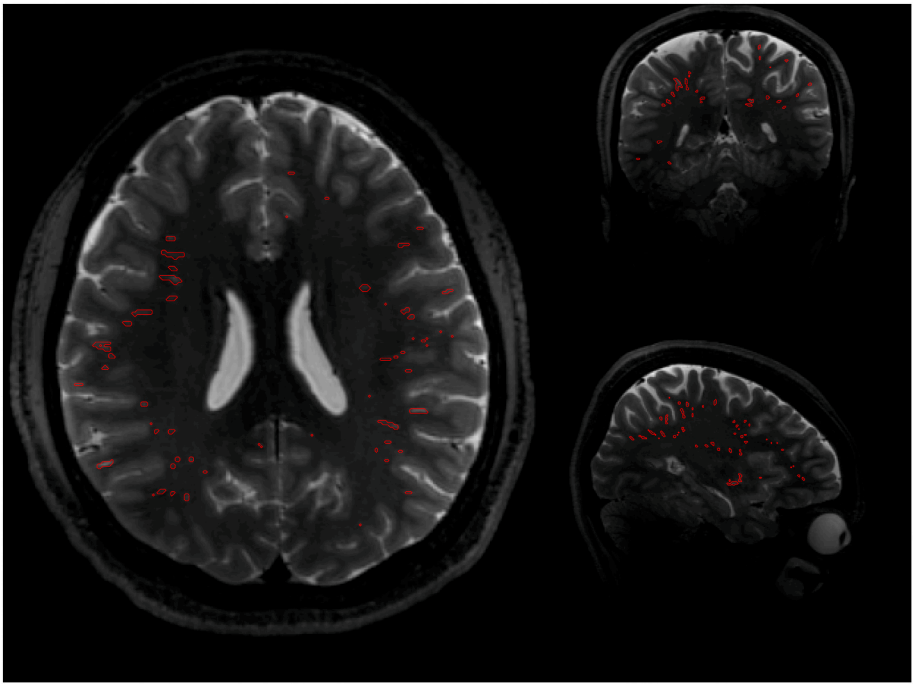

Fig. 2. Example of PVS segmentation result. The images demonstrate the output of the automated nnU-Net PVS segmentation on a representative T2w dataset. The red overlays indicate the segmented PVS in all three anatomical planes (axial, coronal, sagittal). (For interpretation of the references to color in this figure legend, the reader is referred to the Web version of this article.)

2.5.3. Peripheral biomarker assessment

Plasma was obtained by centrifuging whole blood at 1500 g for 10 min, aliquoted, and stored at −80 °C until analysis. After collection of all study samples, plasma was thawed and centrifuged at 400 g for 10 min at 4 °C to remove residual debris. Concentrations of circulating mediators were assessed using bead-based multiplex immunoassays (LEGENDplex™, BioLegend, Koblenz, Germany) according to the manufacturer's protocol and as previously described [49,50], with the following panels applied: the Vascular Inflammation Panel, comprising myoglobin, MRP8/14, NGAL, MMP-2, osteopontin (OPN), MPO, serum amyloid A (SAA), IGFBP-4, ICAM-1, VCAM-1, MMP-9, and cystatin C; and the Neuroinflammation Panel, including VILIP-1, CCL2/MCP-1, sTREM-2, BDNF, TGF-β1, VEGF, IL-6, sTREM-1, β-NGF, IL-18, TNF-α, sRAGE, and CX3CL1. The assay is based on fluorescent bead populations coated with capture antibodies specific to each analyte. Following incubation with plasma, biotinylated detection antibodies were added, forming bead–analyte–antibody complexes, which were subsequently labeled with streptavidin–phycoerythrin. Samples were acquired on an Attune NxT flow cytometer (Thermo Fisher Scientific, Dreieich, Germany) and processed using the LEGENDplex Data Analysis Software Suite.

2.5.4. Statistics

All statistical analyses were performed using Python with the statsmodels and seaborn libraries. Prior to analysis, outliers were managed on a per-timepoint basis using the Median Absolute Deviation (MAD) method. Any data point with a modified Z-score greater than 3.5 was excluded from its respective analysis. To assess the effect of time on the outcome measures, we used a Linear Mixed-Effects Model (LMM). In this model, 'time' (0h, 24h, 96h) was modeled as a fixed effect, and a random intercept for 'participant' was included to account for repeated measures and individual baseline differences. The logarithmic transformation of the metric under consideration (e.g. PVS) was applied where necessary to satisfy the assumptions of the LMM regarding normal distribution and homogeneity of variances, thereby ensuring the statistical validity of the analysis. Alpha was set at 0.05 and asterisks indicate level of significance (*$p < 0.05$, **$p < 0.01$, and ***$p < 0.001$) in the realm of our exploratory study.

3. Results

A total of 18 men (60 %) and 12 women (40 %), with a mean age of 28.0 ± 4.7 years were included. Key demographic and baseline characteristics of the study population are summarized in Table 1.

3.1. PVS

We investigated the impact of sleep deprivation and subsequent recovery on PVS volume across the entire brain and separately for white matter, hippocampus and the basal ganglia (see Fig. 3). The total PVS volume in the whole brain increased significantly from baseline to the 24h sleep deprivation timepoint (6711.5 ± 2643.2 mm^3 vs. 7475.3 ± 2545.4 mm^3; $p < 0.001$) and subsequently decreased following the recovery period at 96h (6721.4 ± 2884.5 mm^3; $p < 0.01$). No significant difference was observed between baseline and the 96h recovery timepoint, suggesting a return to baseline. In contrast, white matter PVS volume did not show a significant change after sleep deprivation but did show a significant decrease during recovery (5961.8 ± 2484.1 mm^3 vs. 6662.1 ± 2417.2 mm^3 and 5362.5 ± 2892.6 mm^3; $p < 0.01$ when comparing baseline to after recovery). In the basal ganglia the volume increased significantly from baseline to the 24h sleep deprivation timepoint (530.5 ± 141.4 mm^3 vs. 552.6 ± 133.2 mm^3; $p < 0.05$) and significant decrease between the 24h and 96h timepoints (552.6 ± 133.2 mm^3 vs. 495.9 ± 126.5 mm^3; $p < 0.001$). In addition, a significant decrease was observed between 0h and 96h (530.5 ± 141.4 mm^3 vs. 495.9 ± 126.5 mm^3; $p < 0.05$). The hippocampus showed a significant change after sleep deprivation (10.4 ± 7.1 mm^3 vs. 12.3 ± 6.7 mm^3; $p < 0.05$) but not during recovery.

3.2. QSM

To assess changes in tissue's magnetic susceptibility, particularly

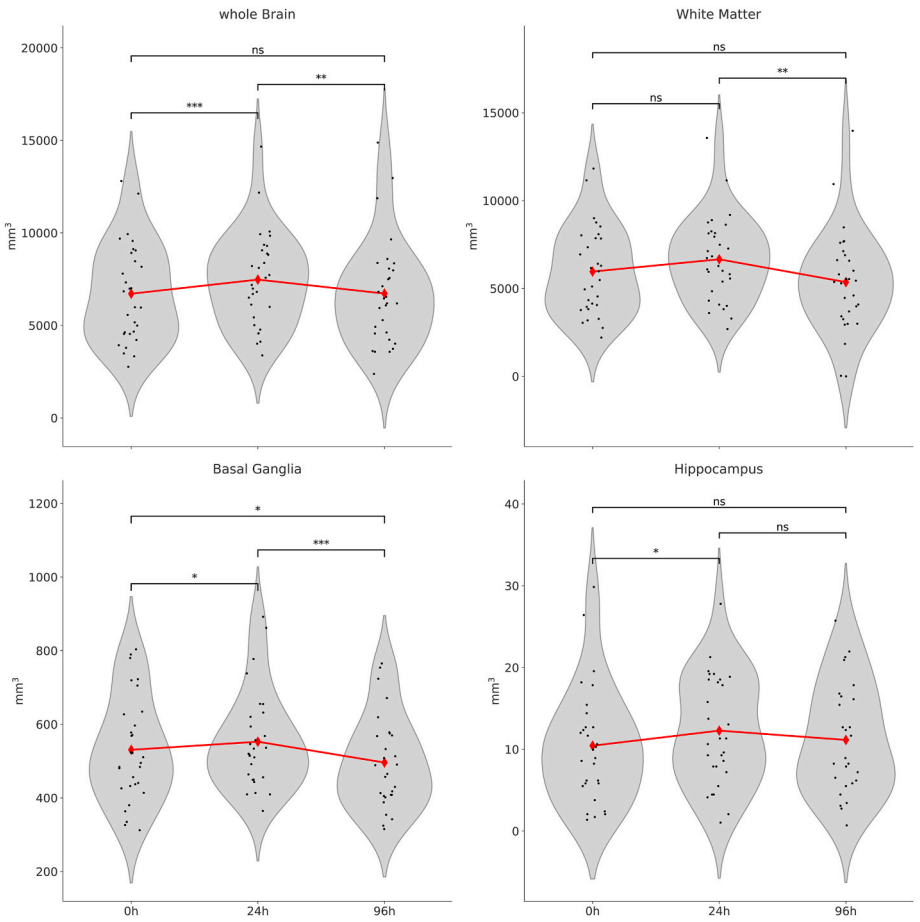

Fig. 3. PVS volume changes following sleep deprivation and recovery. Violin plots show the distribution of data points for each timepoint. Statistical comparisons were performed using a linear mixed-effects model. Significance levels are denoted as ns (not significant), * ($p < 0.05$), ** ($p < 0.01$) and *** ($p < 0.001$).

those related to iron content, we performed QSM (see Fig. 4). The analysis revealed a significant decrease in magnetic susceptibility following 24h of sleep deprivation in several key brain regions. Specifically, susceptibility was significantly changed in the cerebral white matter (-0.0049 ± 0.0017 vs. -0.0053 ± 0.0016; $p < 0.05$), cerebral cortex (-0.0003 ± 0.0013 vs. $6.4378*10^{-5} \pm 0.0014$; $p < 0.01$), cerebellar white matter (0.00185 ± 0.00263 vs. 0.00223 ± 0.00256; $p < 0.05$), pallidum (0.08242 ± 0.00381 vs. 0.08418 ± 0.0143; $p < 0.01$) and ventral diencephalon (ventralDC) (0.00495 ± 0.00523 vs. 0.00585 ± 0.00504; $p < 0.05$). Other regions were also examined, but did not show any significant changes (see Supplementary data).

3.3. T1 relaxation time

To further probe tissue property changes, we analyzed the MP2RAGE-based maps of T1 relaxation time (see Fig. 5). Sleep deprivation induced a significant decrease in T1 relaxation times in several cortical and subcortical grey matter regions. At the 24h timepoint, values of T1 time were significantly reduced in the cerebellar and cerebral cortex (1990.3 ± 52.3 ms vs. 1975.5 ± 43.5 ms and 1951.1 ± 42 vs. 1942.8 ± 40.5 ms; $p < 0.05$ each), hippocampus (1862.4 ± 76.8 ms vs. 1849.5 ± 57.1 ms; $p < 0.05$), inferior lateral ventricle (Inf-Lat-Vent) (2798.8 ± 140.2 ms vs. 2761.2 ± 141.4 ms; $p < 0.001$), pallidum (1177.7 ± 37.2 ms vs. 1174.4 ± 36.4 ms; $p < 0.05$) and thalamus proper (1323.6 ± 36.6 ms vs. 1316.7 ± 33.1 ms; $p < 0.01$). In the cerebellar cortex (1996.9 ± 43 ms; $p < 0.001$), hippocampus (1864.9 ± 60.9 ms; $p < 0.05$), Inf-Lat-Vent (2799.9 ± 124.7 ms; $p < 0.001$) and thalamus proper (1324.6 ± 33.9 ms; $p < 0.001$), these values subsequently increased significantly after the recovery phase at 96h when compared to after sleep deprivation. Other regions did not show any changes over time (see Supplementary data).

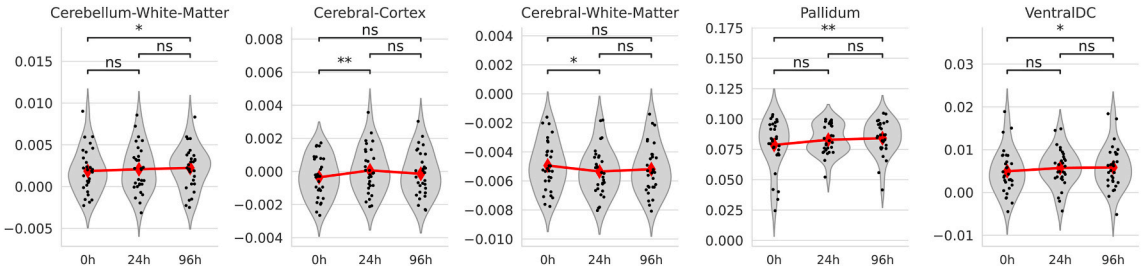

Fig. 4. Regional brain changes in Quantitative Susceptibility Mapping (QSM). Violin plots show the distribution of mean QSM data points for each timepoint. Statistical comparisons were performed using a linear mixed-effects model. Significance levels are denoted as ns (not significant), * ($p < 0.05$), and ** ($p < 0.01$).

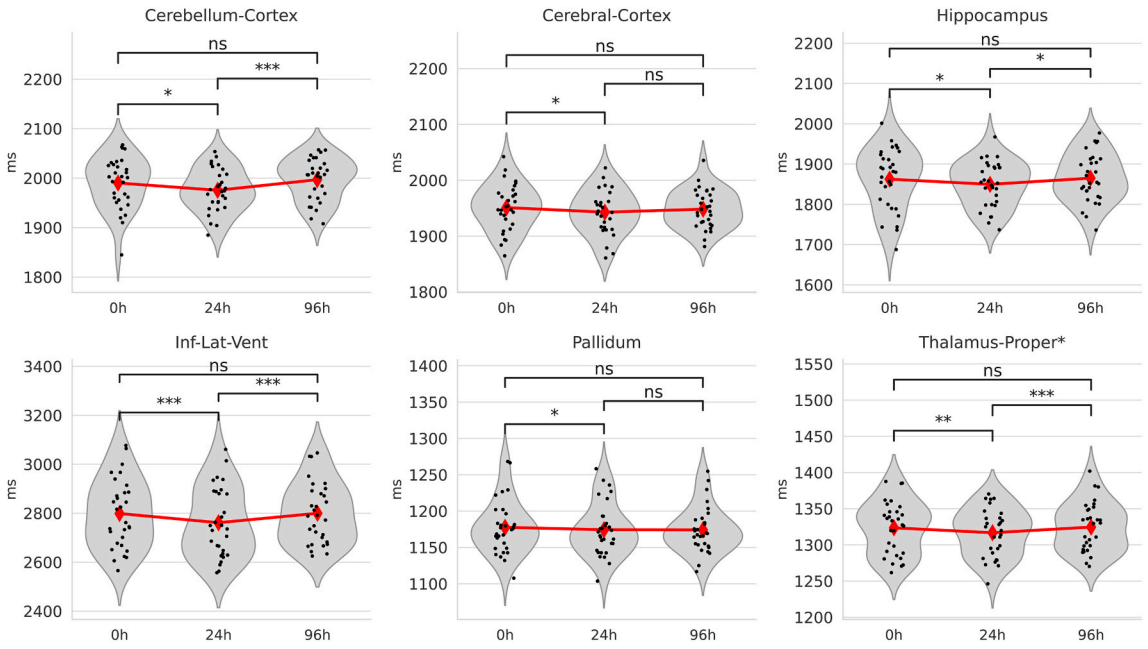

Fig. 5. Regional brain changes in quantitative T1 relaxation times.Violin plots show the distribution of mean T1 data points for each timepoint. Statistical comparisons were performed using a linear mixed-effects model. Significance levels are denoted as ns (not significant), * ($p < 0.05$), ** ($p < 0.01$) and *** ($p < 0.001$).

3.4. NASA PVT

To assess the behavioral impact of sleep deprivation, we analyzed the performance on the PVT (see Fig. 6). While the mean reaction time showed no significant changes across the study duration, a more detailed analysis revealed specific deficits in sustained attention. The reaction times of the slowest 10 % of responses, indicative of attentional lapses, were significantly prolonged at the 24h sleep deprivation timepoint compared to the 12h mark (386.4 ± 59.1 ms vs. 410 ± 74.7 ms; $p < 0.05$). This performance deficit was subsequently reversed following the recovery period, with reaction times at 96h being significantly faster than at 24h (410 ± 74.7 ms vs. 391.1 ± 54 ms; $p < 0.05$). The fastest 10 % of responses showed a slight but significant slowing at 24h compared to baseline (280.7 ± 18.3 ms vs. 289.8 ± 24.4 ms; $p < 0.05$).

3.5. Peripheral biomarker analysis

To investigate the systemic response to sleep deprivation, we analyzed a panel of plasma biomarkers reflecting neurotrophic support, vascular dynamics, tissue remodeling, and inflammation (see Figs. 7 and 8). The results revealed a heterogeneous systemic response with distinct timelines for different markers. Following 24h of sleep deprivation, we observed a significant increase in factors associated with neuroplasticity and neurovascular dynamics, potentially indicating an adaptive response (see Fig. 7). Brain-Derived Neurotrophic Factor (BDNF), β-Nerve Growth Factor (β-NGF) and Vascular Endothelial Growth Factor (VEGF) were all significantly elevated at the 24h timepoint compared to baseline (179.5 ± 27 pg/mL vs. 231.9 ± 38.9 pg/mL, 5.4 ± 1.1 pg/mL vs. 5.9 ± 1.7 pg/mL and 3.5 ± 0.5 pg/mL vs. 5.3 ± 3.1 pg/mL; $p < 0.05$ each). In parallel, we observed dynamic changes in markers related to vascular function and tissue remodeling (see Fig. 8). Osteopontin (OPN) significantly decreased from baseline to 24h (315 ± 94.1 pg/mL vs. 275.3 ± 80 pg/mL; $p < 0.01$) before increasing during recovery (317.1 ± 93.6 pg/mL; $p < 0.01$), while Matrix Metalloproteinase-9 (MMP-9) increased after sleep deprivation (52.3 ± 14.5 pg/mL vs. 69.2 ± 23.5 pg/mL; $p < 0.05$) and decreased after the recovery phase (54.6 ± 16.4 pg/mL; $p < 0.05$). Finally, several markers associated with inflammation and cellular stress exhibited a delayed response, with significant increases occurring primarily after the recovery period. Myeloperoxidase (MPO) and Cystatin C significantly increased after the recovery phase compared to both sleep deprivation and baseline (MPO: 249.6 ± 34.7 pg/mL vs. 228.6 ± 25.4 pg/mL and 219.6 ± 24.5 pg/ml; Cystatin C: 1927.6 ± 617.9 pg/mL vs. 1760.4 ± 477.7 pg/mL and 1781.1 ± 478.9 pg/ml, respectively; $p < 0.05$ for all comparisons). Similarly, myoglobin

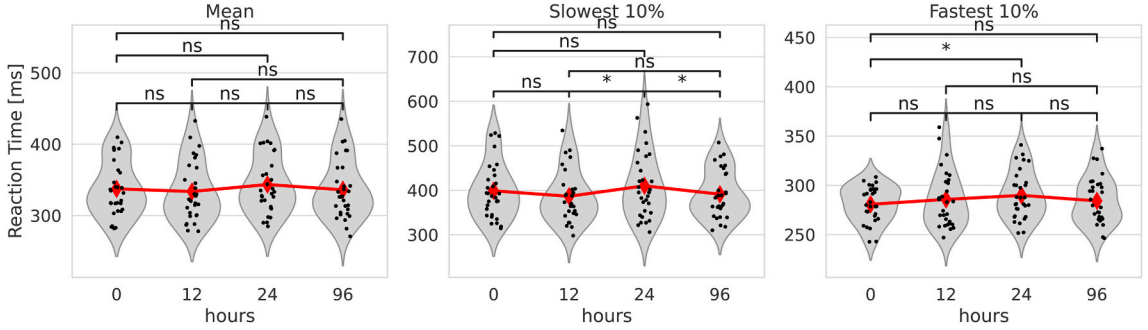

Fig. 6. Psychomotor Vigilance Task (PVT) performance across timepoints. The figure displays the mean reaction time, as well as the slowest 10 % and fastest 10 % of responses, which are indicative of attentional lapses. Statistical comparisons were performed using a linear mixed-effects model. Significance levels are denoted as ns (not significant) and * ($p < 0.05$).

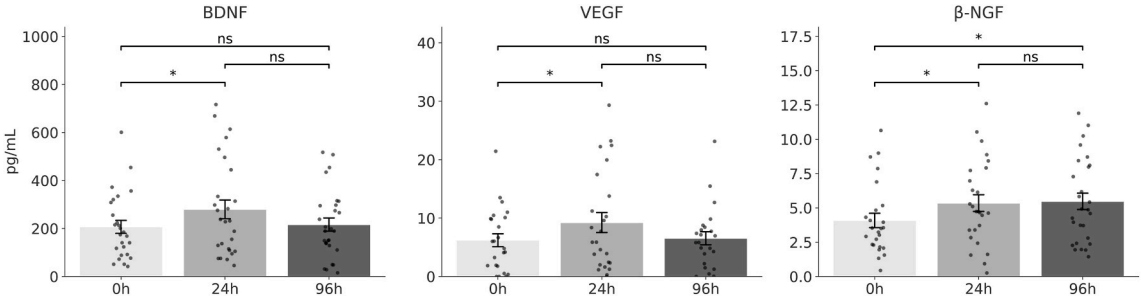

Fig. 7. Plasma concentrations of BDNF, VEGF and β-NGF. Data are presented as individual measurements, with bars indicating the group mean and error bars representing the standard error of the mean. Statistical significance was determined using a linear mixed-effects model. Significance levels: ns (not significant), * ($p < 0.05$).

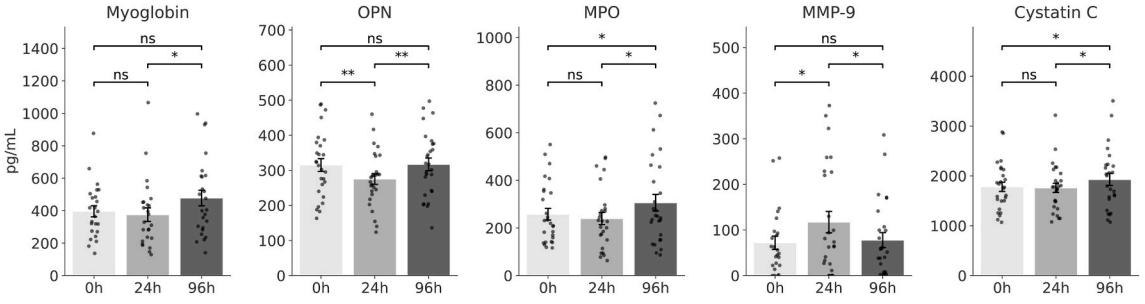

Fig. 8. Plasma concentrations of Myoglobin, OPN, MPO, MMP-9 and Cyastin C.Data are presented as individual measurements, with bars indicating the group mean and error bars representing the standard error of the mean. Statistical significance was determined using a linear mixed-effects model. Significance levels: ns (not significant), * ($p < 0.05$), ** ($p < 0.01$).

increased during the recovery phase compared to after sleep deprivation (329.2 ± 41.7 pg/mL vs. 478 ± 239 pg/mL; $p < 0.05$). All other markers did not show significant changes over time (see Supplementary data).

3.6. Correlation network analysis of multimodal changes

Correlation network analysis (see Fig. 9) showed numerous strong, mainly positive Pearson's correlations after 24h sleep deprivation, particularly within neuroanatomical variables. QSM and T1 metrics formed dense, highly intercorrelated clusters ($|r| > 0.6$), including central PVS-associated nodes, indicating a global, synchronous volumetric response. In contrast, blood biomarkers and PVT measures showed few strong correlations and remained largely isolated.

During recovery (Δ 96h–24h), the network reorganized substantially. Dense QSM clusters and tight PVS couplings dissolved, suggesting decoupling and normalization. New, distinct correlations appeared within T1 measures, consistent with regenerative processes. PVT and blood measures remained isolated.

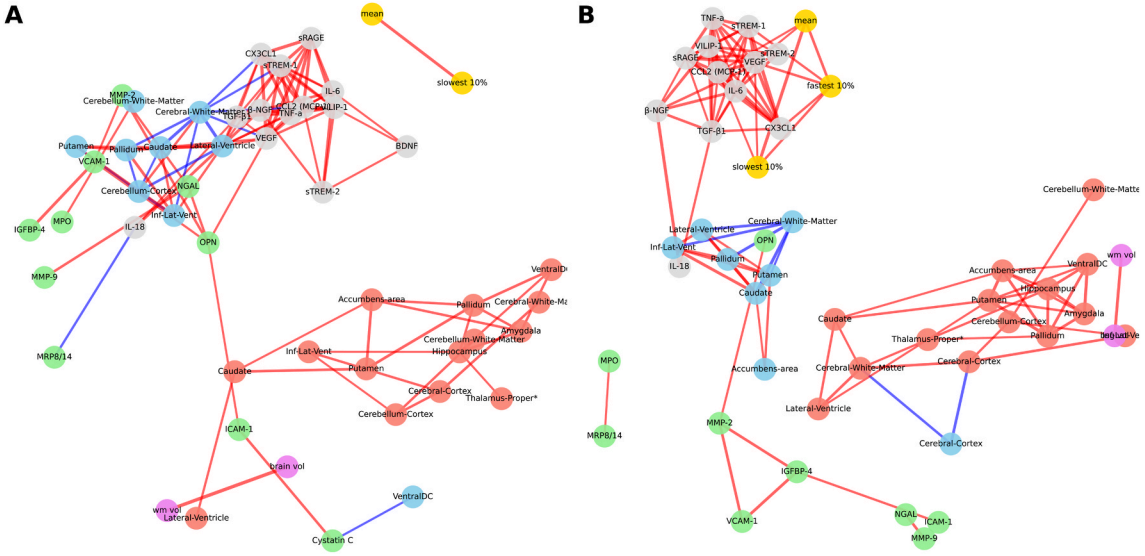

Fig. 9. Biomarker and brain morphometry correlation networks. The networks display significant Pearson's correlations ($|corr| > 0.6$) in A (Δ24h-0h) and B (Δ96h-24h). Nodes are colored by modality (PVS: violet; QSM: blue; T1: red; vascular blood: green; neuro blood: grey; PVT: yellow). Lines indicate a significant positive (red) or negative (blue) correlation, with line thickness representing the correlation strength. (For interpretation of the references to color in this figure legend, the reader is referred to the Web version of this article.)

4. Discussion

The most direct indication of impaired glymphatic clearance is the significant increase in total PVS volume after 24h of sleep deprivation. PVS are an essential component of the glymphatic system, and their enlargement indicates impaired drainage and a resulting accumulation of interstitial fluid [51,52]. The fact that this volume completely normalized after a three-day recovery period underscores the reversibility of this process and the ability to restore homeostasis. The regional heterogeneity of the changes, with clear effects throughout the brain, basal ganglia and the hippocampus, suggests that different areas of the brain have different levels of vulnerability, which might be due to differences in metabolic activity, vascular density or susceptibility [53].

Particularly revealing was the inverse relationship between PVS increase and significant shortening of T1 relaxation times in several cortical and subcortical regions after sleep deprivation. This finding indicates acute tissue dehydration and supports the hypothesis of fluid shift from the brain parenchyma into the expanding PVS. The overshoot measurable after the recovery phase indicates compensatory rehydration and underscores the elasticity of the osmotic balance. In addition, QSM measurements showed small, equally reversible shifts in magnetic susceptibility, which are likely due to temporary changes in local water and iron content as a result of osmotic stress. There was a slight decrease in cerebral white matter, consistent with water retention due to simultaneous PVS dilation. The inverse correlation between Δ24/0-PVS and Δ24/0-QSM-white matter supports this fluid shift model. Overall, QSM shows that even a single sleepless night triggers measurable but completely reversible micro changes without indicating structural damage.

Our correlation network analysis (Fig. 9) provides further support for this model of a global fluid shift. After 24h of sleep deprivation (Δ24h-0h), we observed a dense clustering of PVS, T1, and QSM metrics, suggesting a global, synchronous physiological event consistent with a widespread fluid shift. This tight coupling almost completely dissolved during the recovery phase (Δ96h-24h), indicating a 'decoupling' and normalization of these individual components as homeostasis was restored. This network-level reorganization from a highly correlated state (stress) to a sparse state (recovery) aligns with our interpretation of a transient, fully reversible physiological cascade.

The results of our peripheral biomarker analysis complement these imaging findings, offering insights into the complex systemic response to sleep deprivation. The transient increase in MMP-9 following 24h of sleep deprivation is particularly noteworthy. Given that MMP-9 is known to modulate the function of aquaporin-4 (AQP4) water channels, which are integral to glymphatic transport [54], this finding may offer a potential mechanistic link to our observation of PVS enlargement. While long-term elevation of MMP-9 is associated with pathology [54], its acute increase here could speculatively contribute to a temporary disruption in glymphatic clearance. Beyond MMP-9, the biomarker panel revealed a multi-faceted response with distinct temporal profiles, rather than a simple inflammatory cascade. The immediate rise in neurotrophic factors, including BDNF and β-NGF, is likely not a sign of neuroinflammation but rather an adaptive plasticity response, possibly aimed at promoting cellular resilience against the stress of sleep loss. This initial neuroprotective signature was contrasted by changes in vascular and stress-related markers. The dynamic shifts in VEGF and OPN underscore the concurrent impact on neurovascular dynamics. Furthermore, the delayed increase of the pro-inflammatory marker MPO and tissue stress markers like myoglobin and Cystatin C, which peaked only after the recovery period, suggests a second wave of metabolic and cellular stress that persists even after sleep is resumed. Collectively, these findings delineate a biphasic systemic response characterized by an initial, adaptive neurotrophic phase that is succeeded by a prolonged period of systemic vascular and metabolic stress.

Finally, this physiological cascade manifests itself at the functional level [55]. Although the average reaction time remained unaffected, sleep deprivation led to a significant slowing of the slowest 10 % of responses in the PVT, a classic sign of increased attention deficits ("lapses") [56]. This cognitive impairment, which returned to normal [57] in parallel with the physiological markers, can be considered a direct behavioral correlate of disturbed cerebral homeostasis.

In summary, our multimodal findings deliver a coherent picture: 24h of sleep deprivation seems to primarily disrupt glymphatic function, which is reflected in PVS enlargement. This is accompanied by secondary, dynamic fluid shifts and microstructural adaptations that can be detected using quantitative T1 and QSM imaging. An increase in MMP-9 provides a possible mechanistic explanation, while vigilancetests reveal the functional deficit of this cascade. The complete reversibility of these effects underscores the resilience of the young, healthy brain.

5. Limitations

Our study has limitations. First, a longer sleep deprivation phase and several MRIs to monitor progression would have been more helpful to elicit detailed dynamic information for changes. For example, it would allow us to see if the changes (e.g. in PVS) plateau after 24h or continue to worsen, providing greater insight into the *rate* of change and the coping capacity of the system. However, the participants' discomfort with longer periods without sleep and the repetitive MRI scans also needed to be considered; therefore, we chose to compromise. Second, although the participants were verbally instructed not to consume alcohol and to avoid caffeine consumption that could affect their routine sleep-wake cycle and glymphatic activity, we cannot rule this out completely as they were not strictly watched or recorded during the recovery phase. Third, we did not track the subjects' sleep either before the start of sleep deprivation or afterwards and therefore cannot draw any conclusions about sleep quality and immediate sleep behavior. Fourth, as this was an exploratory study combining novel 7T MRI, biomarker etc, a formal a priori power analysis was not performed. Fifthly, with regard to the PVT results, it cannot be ruled out that a training effect may have had an impact on the test subjects. The test subjects carried out a demo session before the start, but it can be assumed that the test subjects were prepared for the test at different speeds and to different degrees. Lastly, it remains unclear whether our findings are valid in elderly people or patients with disease affecting brain homeostasis. Further studies are warranted to investigate the effects of sleep deprivation in such cohorts.

6. Conclusions

Sleep deprivation leads to rapid, reversible changes in PVS volume, which are linked to microstructural tissue changes detectable with quantitative MRI. Systemic inflammatory markers and sustained attention measures provide additional evidence. These findings reinforce the concept that glymphatic function is a central regulator of sleep-dependent brain homeostasis.

CRediT authorship contribution statement

Eric Einspänner: Writing – original draft, Visualization, Validation, Software, Methodology, Formal analysis, Data curation, Conceptualization. **Hendrik Mattern:** Writing – review & editing, Methodology, Formal analysis. **Heiko Grossmann:** Writing – review & editing, Formal analysis. **Eya Khadhraoui:** Writing – review & editing, Data curation. **Sebastian J. Müller:** Writing – review & editing, Data curation. **Alejandra P. Garza:** Writing – review & editing, Data curation. **Ildiko R. Dunay:** Writing – review & editing, Supervision, Funding acquisition, Data curation. **Katharina Schregel:** Writing – review & editing, Visualization. **Charles R.G. Guttmann:** Writing – review & editing. **Erelle Fuchs:** Writing – review & editing, Project administration, Methodology, Data curation, Conceptualization. **Daniel Behme:** Writing – review & editing, Supervision, Project administration, Formal analysis,

Conceptualization.

Funding sources/financial disclosure

This research did not receive any specific grant from funding agencies in the public, commercial, or not-for-profit sectors.

K.S. was supported by the Else Kröner-Fresenius-Stiftung (2023_EKEA.53).

Declaration of competing interest

The authors declare that they have no known competing financial interests or personal relationships that could have appeared to influence the work reported in this paper.

Acknowledgements

We thank Cindy Lübeck and Niklas Kelling from the Department of Biomedical Magnetic Resonance (BMMR), OvGU, Magdeburg, for their assistance with the 7T MRI data acquisition. This study was supported by funding from the Medical Faculty, OvGU, Magdeburg.

Appendix A. Supplementary data

Supplementary data to this article can be found online at https://doi.org/10.1016/j.sleep.2025.108663.

References

[1] Xie L, et al. Sleep drives metabolite clearance from the adult brain. Sci Oct. 2013; 342(6156):373–7. https://doi.org/10.1126/science.1241224.

[2] Rasmussen MK, Mestre H, Nedergaard M. Fluid transport in the brain. Physiol Rev Apr. 2022;102(2):1025–151. https://doi.org/10.1152/physrev.00031.2020.

[3] Dredla BK, Del Brutto OH, Castillo PR. Sleep and perivascular spaces. Curr Neurol Neurosci Rep Oct. 2023;23(10):607–15. https://doi.org/10.1007/s11910-023-01293-z.

[4] Astara K, et al. A novel conceptual framework for the functionality of the glymphatic system. J Neurophysiol May 2023;129(5):1228–36. https://doi.org/10.1152/jn.00360.2022.

[5] Wang X-X, et al. MRI-visible enlarged perivascular spaces: imaging marker to predict cognitive impairment in older chronic insomnia patients. Eur Radiol Aug. 2022;32(8):5446–57. https://doi.org/10.1007/s00330-022-08649-y.

[6] Wardlaw JM, et al. Perivascular spaces in the brain: anatomy, physiology and pathology. Nat Rev Neurol Mar. 2020;16(3):137–53. https://doi.org/10.1038/s41582-020-0312-z.

[7] Agarwal N, et al. Current understanding of the anatomy, physiology, and magnetic resonance imaging of neurofluids: update from the 2022 ' ISMRM Imaging Neurofluids Study group' workshop in rome. J Magn Reson Imag Feb. 2024;59(2): 431–49. https://doi.org/10.1002/jmri.28759.

[8] Oltmer J, et al. Enlarged perivascular spaces in the basal ganglia are associated with arteries not veins. J Cerebr Blood Flow Metabol Nov. 2024;44(11):1362–77. https://doi.org/10.1177/0271678X241260629.

[9] Scalise A, et al. Increasing cortical excitability: a possible explanation for the proconvulsant role of sleep deprivation. Sleep Dec. 2006;29(12):1595–8. https://doi.org/10.1093/sleep/29.12.1595.

[10] Aydın S. Computer based synchronization analysis on sleep EEG in insomnia. J Med Syst Aug. 2011;35(4):517–20. https://doi.org/10.1007/s10916-009-9387-1.

[11] Aydın S, Tunga MA, Yetkin S. Mutual information analysis of sleep EEG in detecting psycho-physiological insomnia. J Med Syst May 2015;39(5):43. https://doi.org/10.1007/s10916-015-0219-1.

[12] Dai X-J, Zhang J, Wang Y, Ma Y, Shi K. Editorial: EEG and fMRI for sleep and sleep disorders–mechanisms and clinical implications. Front Neurol Sept. 2021;12: 749620. https://doi.org/10.3389/fneur.2021.749620.

[13] Bishir M, et al. Sleep deprivation and neurological disorders. BioMed Res Int Jan. 2020;2020(1):5764017. https://doi.org/10.1155/2020/5764017.

[14] Di Meco A, Joshi YB, Praticò D. Sleep deprivation impairs memory, tau metabolism, and synaptic integrity of a mouse model of Alzheimer's disease with plaques and tangles. Neurobiol Aging Aug. 2014;35(8):1813–20. https://doi.org/10.1016/j.neurobiolaging.2014.02.011.

[15] Zhu B, et al. Sleep disturbance induces neuroinflammation and impairment of learning and memory. Neurobiol Dis Dec. 2012;48(3):348–55. https://doi.org/10.1016/j.nbd.2012.06.022.

[16] Wang C, et al. Chronic sleep deprivation exacerbates cognitive and synaptic plasticity impairments in APP/PS1 transgenic mice. Behav Brain Res Aug. 2021; 412:113400. https://doi.org/10.1016/j.bbr.2021.113400.

[17] Qiu H, Zhong R, Liu H, Zhang F, Li S, Le W. Chronic sleep deprivation exacerbates learning-memory disability and alzheimer's disease-like pathologies in AβPPswe/PS1ΔE9 mice. J Alzheimers Dis Feb. 2016;50(3):669–85. https://doi.org/10.3233/JAD-150774.

[18] Baril A-A, et al. Lighter sleep is associated with higher enlarged perivascular spaces burden in middle-aged and elderly individuals. Sleep Med Dec. 2022;100:558–64. https://doi.org/10.1016/j.sleep.2022.10.006.

[19] S. P. Gunawan et al., "Chronic sleep deprivation is associated with delayed puberty onset in rats, activation of proinflammatory cytokines and gut dysbiosis".

[20] Ballesio A, Fiori V, Lombardo C. Effects of experimental sleep deprivation on peripheral inflammation: an updated meta-analysis of human studies. J Sleep Res June 2025:e70099. https://doi.org/10.1111/jsr.70099.

[21] Pham W, et al. A critical guide to the automated quantification of perivascular spaces in magnetic resonance imaging. Front Neurosci Dec. 2022;16:1021311. https://doi.org/10.3389/fnins.2022.1021311.

[22] Barisano G, et al. Imaging perivascular space structure and function using brain MRI. Neuroimage Aug. 2022;257:119329. https://doi.org/10.1016/j.neuroimage.2022.119329.

[23] Bacyinski A, Xu M, Wang W, Hu J. The paravascular pathway for brain waste clearance: current understanding, significance and controversy. Front Neuroanat Nov. 2017;11:101. https://doi.org/10.3389/fnana.2017.00101.

[24] Kwee RM, Kwee TC. Virchow-robin spaces at MR imaging. Radiographics July 2007;27(4):1071–86. https://doi.org/10.1148/rg.274065722.

[25] Bouvy WH, Biessels GJ, Kuijf HJ, Kappelle LJ, Luijten PR, Zwanenburg JJM. Visualization of perivascular spaces and perforating arteries with 7 T magnetic resonance imaging. Investig Radiol May 2014;49(5):307–13. https://doi.org/10.1097/RLI.0000000000000027.

[26] Barisano G, Law M, Custer RM, Toga AW, Sepehrband F. Perivascular space imaging at ultrahigh field MR imaging. Magn Reson Imag Clin N Am Feb. 2021;29 (1):67–75. https://doi.org/10.1016/j.mric.2020.09.005.

[27] Hou Y, et al. Enhancement of perivascular spaces in 7 T MR image using haar transform of non-local cubes and block-matching filtering. Sci Rep Aug. 2017;7(1): 8569. https://doi.org/10.1038/s41598-017-09336-5.

[28] Lian C, Liu M, Zhang J, Zong X, Lin W, Shen D. "Automatic Segmentation of 3D Perivascular Spaces in 7T MR Images Using Multi-Channel Fully Convolutional Network,". 2018.

[29] Voorter PHM, et al. Blood–brain barrier disruption and perivascular spaces in small vessel disease and neurodegenerative diseases: a review on MRI methods and insights. J Magn Reson Imag Feb. 2024;59(2):397–411. https://doi.org/10.1002/jmri.28989.

[30] D. Neary, A. Jackson, T. F. Patankar, D. Mitra, and A. Varma, "Dementia disease: study in elderly patients with sensitive indicator of cerebral microvascular dilatation of the virchow-robin space is a".

[31] Chen W, Song X, Zhang Y. And for the alzheimer's disease neuroimaging initiative, "Assessment of the Virchow-Robin Spaces in Alzheimer Disease, Mild Cognitive Impairment, and Normal Aging, Using High-Field MR Imaging,". Am J Neuroradiol Sept. 2011;32(8):1490–5. https://doi.org/10.3174/ajnr.A2541.

[32] Laveskog A, Wang R, Bronge L, Wahlund L-O, Qiu C. Perivascular spaces in old age: assessment, distribution, and correlation with white matter hyperintensities. Am J Neuroradiol Jan. 2018;39(1):70–6. https://doi.org/10.3174/ajnr.A5455.

[33] Alhola P, Polo-Kantola P. Sleep deprivation: impact on cognitive performance. Neuropsychiatric Dis Treat 2007;3(5):553–67.

[34] Custer RM, et al. Effects of one-night partial sleep deprivation on perivascular space volume fraction: findings from the Stockholm sleepy brain study. Neuroscience Oct. 27, 2024. https://doi.org/10.1101/2024.10.26.620382.

[35] Eckstein K, et al. Computationally efficient combination of multi-channel phase data from multi-echo acquisitions (ASPIRE). Magn Reson Med June 2018;79(6): 2996–3006. https://doi.org/10.1002/mrm.26963.

[36] Dinges DF, Powell JW. Microcomputer analyses of performance on a portable, simple visual RT task during sustained operations. Behav Res Methods Instrum Comput Nov. 1985;17(6):652–5. https://doi.org/10.3758/BF03200977.

[37] Arsintescu L, Kato KH, Cravalho PF, Feick NH, Stone LS, Flynn-Evans EE. Validation of a touchscreen psychomotor vigilance task. Accid Anal Prev May 2019;126:173–6. https://doi.org/10.1016/j.aap.2017.11.041.

[38] Isensee F, Jaeger PF, Kohl SAA, Petersen J, Maier-Hein KH. nnU-Net: a self-configuring method for deep learning-based biomedical image segmentation. Nat Methods Feb. 2021;18(2):203–11. https://doi.org/10.1038/s41592-020-01008-z.

[39] Huang P, et al. Development and validation of a perivascular space segmentation method in multi-center datasets. Neuroimage Sept. 2024;298:120803. https://doi.org/10.1016/j.neuroimage.2024.120803.

[40] Cai D, et al. Deep-learning-based segmentation of perivascular spaces on T2-Weighted 3T magnetic resonance images. Front Aging Neurosci Aug. 2024;16: 1457405. https://doi.org/10.3389/fnagi.2024.1457405.

[41] Fedorov A, et al. 3D slicer as an image computing platform for the quantitative imaging network. Magn Reson Imaging Nov. 2012;30(9):1323–41. https://doi.org/10.1016/j.mri.2012.05.001.

[42] Pinter C, Lasso A, Fichtinger G. Polymorph segmentation representation for medical image computing. Comput Methods Progr Biomed Apr. 2019;171:19–26. https://doi.org/10.1016/j.cmpb.2019.02.011.

[43] Pérez-García F, Sparks R, Ourselin S. TorchIO: a python library for efficient loading, preprocessing, augmentation and patch-based sampling of medical images in deep learning. Comput Methods Progr Biomed Sept. 2021;208:106236. https://doi.org/10.1016/j.cmpb.2021.106236.

[44] Klein A, Tourville J. 101 labeled brain images and a consistent human cortical labeling protocol. Front Neurosci 2012;6. https://doi.org/10.3389/fnins.2012.00171.

[45] Desikan RS, et al. An automated labeling system for subdividing the human cerebral cortex on MRI scans into gyral based regions of interest. Neuroimage July 2006;31(3):968–80. https://doi.org/10.1016/j.neuroimage.2006.01.021.
[46] Acosta-Cabronero J, Milovic C, Mattern H, Tejos C, Speck O, Callaghan MF. A robust multi-scale approach to quantitative susceptibility mapping. Neuroimage Dec. 2018;183:7–24. https://doi.org/10.1016/j.neuroimage.2018.07.065.
[47] Henschel L, Conjeti S, Estrada S, Diers K, Fischl B, Reuter M. FastSurfer - a fast and accurate deep learning based neuroimaging pipeline. Neuroimage Oct. 2020;219:117012. https://doi.org/10.1016/j.neuroimage.2020.117012.
[48] Jenkinson M, Bannister P, Brady M, Smith S. Improved optimization for the robust and accurate linear registration and motion correction of brain images. Neuroimage Oct. 2002;17(2):825–41. https://doi.org/10.1006/nimg.2002.1132.
[49] Besteher B, et al. Cortical thickness alterations and systemic inflammation define long-COVID patients with cognitive impairment. Brain Behav Immun Feb. 2024;116:175–84. https://doi.org/10.1016/j.bbi.2023.11.028.
[50] Garza AP, et al. Initial and ongoing tobacco smoking elicits vascular damage and distinct inflammatory response linked to neurodegeneration. Brain Behav Immun - Health Mar. 2023;28:100597. https://doi.org/10.1016/j.bbih.2023.100597.
[51] Yu L, Hu X, Li H, Zhao Y. Perivascular spaces, glymphatic system and MR. Front Neurol May 2022;13:844938. https://doi.org/10.3389/fneur.2022.844938.
[52] Bohr T, et al. The glymphatic system: current understanding and modeling. iScience Sept. 2022;25(9):104987. https://doi.org/10.1016/j.isci.2022.104987.
[53] Shih N-C, Barisano G, Lincoln KD, Mack WJ, Sepehrband F, Choupan J. Effects of sleep on brain perivascular space in a cognitively healthy population. Sleep Med Nov. 2023;111:170–9. https://doi.org/10.1016/j.sleep.2023.09.024.
[54] Si X, et al. Matrix metalloproteinase-9 inhibition prevents aquaporin-4 depolarization-mediated glymphatic dysfunction in Parkinson's disease. J Adv Res Feb. 2024;56:125–36. https://doi.org/10.1016/j.jare.2023.03.004.
[55] Xu Z, et al. Dynamic changes in brain function during sleep deprivation: increased occurrence of non-stationary states indicates the extent of cognitive impairment. Neuroimage Apr. 2025;309:121099. https://doi.org/10.1016/j.neuroimage.2025.121099.
[56] Cain SW, Silva EJ, Chang A-M, Ronda JM, Duffy JF. One night of sleep deprivation affects reaction time, but not interference or facilitation in a stroop task. Brain Cognit June 2011;76(1):37–42. https://doi.org/10.1016/j.bandc.2011.03.005.
[57] Antler CA, Yamazaki EM, Casale CE, Brieva TE, Goel N. The 3-Minute psychomotor vigilance test demonstrates inadequate convergent validity relative to the 10-Minute psychomotor vigilance test across sleep loss and recovery. Front Neurosci Feb. 2022;16:815697. https://doi.org/10.3389/fnins.2022.815697.